

# Magnetic field sensor using tilted fiber grating interacting with magnetic fluid

Zheng, Jie; Dong, Xinyong; Zu, Peng; Shao, Li-Yang; Chan, Chi Chiu; Cui, Ying; Shum, Perry  
Ping

2013

Zheng, J., Dong, X., Zu, P., Shao, L. Y., Chan, C. C., Cui, Y., & Shum, P. P. (2013). Magnetic field sensor using tilted fiber grating interacting with magnetic fluid. *Optics Express*, 21(15), 17863-17868.

<https://hdl.handle.net/10356/98154>

<https://doi.org/10.1364/OE.21.017863>

---

© 2013 OSA. This paper was published in *Optics Express* and is made available as an electronic reprint (preprint) with permission of OSA. The paper can be found at the following official DOI: [<http://dx.doi.org/10.1364/OE.21.017863>]. One print or electronic copy may be made for personal use only. Systematic or multiple reproduction, distribution to multiple locations via electronic or other means, duplication of any material in this paper for a fee or for commercial purposes, or modification of the content of the paper is prohibited and is subject to penalties under law.

*Downloaded on 25 Aug 2022 01:40:38 SGT*

# Magnetic field sensor using tilted fiber grating interacting with magnetic fluid

Jie Zheng,<sup>1,2,3</sup> Xinyong Dong,<sup>1,3,4,\*</sup> Peng Zu,<sup>5</sup> Li-Yang Shao,<sup>1</sup> Chi Chiu Chan,<sup>5</sup>  
Ying Cui,<sup>2,3</sup> and Perry Ping Shum<sup>2,3</sup>

<sup>1</sup>Institute of Optoelectronic Technology, China Jiliang University, Hangzhou 310018, China

<sup>2</sup>School of Electrical and Electronics Engineering, Nanyang Technological University, Singapore 639798, Singapore

<sup>3</sup>CINTRA, Research Techno Plaza, 50 Nanyang Drive, Singapore 637553, Singapore

<sup>4</sup>School of Materials Science and Engineering, Nanyang Technological University, Singapore 639798, Singapore

<sup>5</sup>School of Chemical and Biomedical Engineering, Nanyang Technological University, Singapore 637459, Singapore  
[xydong@cjl.u.edu.cn](mailto:xydong@cjl.u.edu.cn)

**Abstract:** A novel magnetic field sensor using tilted fiber Bragg grating (TFBG) interacting with magnetic fluid is proposed and experimentally demonstrated. The TFBG is surrounded by magnetic fluid whose complex refractive index changes with external magnetic field. The guiding properties of cladding modes excited by the TFBG are therefore modulated by the external magnetic field. As a result, the magnetic field strength measurement is successfully achieved within a range up to 196 Gauss by monitoring extinction ratio of cladding mode resonance. Furthermore, temperature variation can be obtained simultaneously from the wavelength shift of the TFBG transmission spectrum.

©2013 Optical Society of America

**OCIS codes:** (280.4788) Optical sensing and sensors; (060.2370) Fiber optics sensors; (060.3735) Fiber Bragg gratings; (230.3810) Magneto-optic systems.

---

## References and links

1. Y. S. Didosyan, H. Hauser, J. Nicolics, V. Y. Barash, and P. L. Fulmek, "Magneto-optical current sensor by domain wall motion in orthoferrites," *IEEE Trans. Instrum. Meas.* **49**(1), 14–18 (2000).
2. N. Itoh, H. Minemoto, D. Ishiko, and S. Ishizuka, "Optical magnetic field sensors with high linearity using bi-substituted rare earth iron garnets," *IEEE Trans. Magn.* **31**(6), 3191–3193 (1995).
3. P. Zu, C. C. Chan, T. Gong, Y. Jin, W. C. Wong, and X. Dong, "Magneto-optical fiber sensor based on bandgap effect of photonic crystal fiber infiltrated with magnetic fluid," *Appl. Phys. Lett.* **101**(24), 241118 (2012).
4. P. Zu, C. C. Chan, W. S. Lew, Y. Jin, Y. Zhang, H. F. Liew, L. H. Chen, W. C. Wong, and X. Dong, "Magneto-optical fiber sensor based on magnetic fluid," *Opt. Lett.* **37**(3), 398–400 (2012).
5. J. Dai, M. Yang, X. Li, H. Liu, and X. Tong, "Magnetic field sensor based on magnetic fluid clad etched fiber Bragg grating," *Opt. Fiber Technol.* **17**(3), 210–213 (2011).
6. T. Hu, Y. Zhao, X. Li, J. Chen, and Z. Lv, "Novel optical fiber current sensor based on magnetic fluid," *Opt. Lett.* **8**(4), 392–394 (2010).
7. L. Martinez, F. Cecelja, and R. Rakowski, "A novel magneto-optic ferrofluid material for sensor applications," *Sens. Actuators A Phys.* **123–124**, 438–443 (2005).
8. S. Y. Yang, J. J. Chieh, H. E. Horng, C. Y. Hong, and H. C. Yang, "Origin and applications of magnetically tunable refractive index of magnetic fluid films," *Appl. Phys. Lett.* **84**(25), 5204–5206 (2004).
9. T. Liu, X. Chen, Z. Di, J. Zhang, X. Li, and J. Chen, "Tunable magneto-optical wavelength filter of long-period fiber grating with magnetic fluids," *Appl. Phys. Lett.* **91**(12), 121116 (2007).
10. S. Pu, X. Chen, L. Chen, W. Liao, Y. Chen, and Y. Xia, "Tunable magnetic fluid grating by applying a magnetic field," *Appl. Phys. Lett.* **87**(2), 021901 (2005).
11. P. Childs, A. Candiani, and S. Pissadakis, "Optical fiber cladding ring magnetic field sensor," *IEEE Photon. Technol. Lett.* **23**(13), 929–931 (2011).
12. J. Albert, L. Y. Shao, and C. Caucheteur, "Tilted fiber Bragg grating sensors," *Laser Photon. Rev.* **7**(1), 83–108 (2013).
13. T. Guo, C. Chen, A. Laronche, and J. Albert, "Power-referenced and temperature-calibrated optical fiber refractometer," *IEEE Photon. Technol. Lett.* **20**(8), 635–637 (2008).
14. Y. P. Miao, B. Liu, and Q. Zhao, "Refractive index sensor based on measuring the transmission power of tilted fiber Bragg grating," *Opt. Fiber Technol.* **15**(3), 233–236 (2009).
15. T. Li, X. Dong, C. C. Chan, C. L. Zhao, and S. Jin, "Power-referenced optical fiber refractometer based on a hybrid fiber grating," *IEEE Photon. Technol. Lett.* **23**(22), 1706–1708 (2011).
16. X. Dong, Y. Liu, L. Y. Shao, J. Kang, and C. L. Zhao, "Temperature-independent fiber bending sensor based on a superimposed grating," *IEEE Sens. J.* **11**(11), 3019–3022 (2011).

17. L. Y. Shao and J. Albert, "Lateral force sensor based on a core-offset tilted fiber Bragg grating," *Opt. Commun.* **284**(7), 1855–1858 (2011).
18. T. Guo, L. Shang, Y. Ran, B. O. Guan, and J. Albert, "Fiber-optic vector vibroscope," *Opt. Lett.* **37**(13), 2703–2705 (2012).
19. T. Guo, L. Shao, H. Y. Tam, P. A. Krug, and J. Albert, "Tilted fiber grating accelerometer incorporating an abrupt biconical taper for cladding to core recoupling," *Opt. Express* **17**(23), 20651–20660 (2009).
20. X. Dong, T. Li, Y. Liu, Y. Li, C. L. Zhao, and C. C. Chan, "Polyvinyl alcohol-coated hybrid fiber grating for relative humidity sensing," *J. Biomed. Opt.* **16**(7), 077001 (2011).
21. V. Lucarini, J. J. Saarinen, K.-E. Peiponen, and E. M. Vartiainen, *Kramers-Kronig Relations in Optical Materials Research* (Springer, 2005).
22. W. Zhou, D. J. Mandia, M. B. E. Griffiths, A. Bialiaieu, Y. Zhang, P. G. Gordon, S. T. Barry, and J. Albert, "Polarization-dependent properties of the cladding modes of a single mode fiber covered with gold nanoparticles," *Opt. Express* **21**(1), 245–255 (2013).
23. N. A. Yusuf, A. Ramadan, and H. Abu-Safia, "The wavelength and concentration dependence of the magneto-dielectric anisotropy effect in magnetic fluids determined from magneto-optical measurements," *J. Magn. Magn. Mater.* **184**(3), 375–386 (1998).
24. C. Y. Hong, H. E. Horng, and S. Y. Yang, "Tunable refractive index of magnetic fluids and its applications," *Phys. Status Solidi* **1**(7), 1604–1609 (2004) (c).
25. L.-Y. Shao, J. P. Coyle, S. T. Barry, and J. Albert, "Anomalous permittivity and plasmon resonances of copper nanoparticle conformal coatings on optical fibers," *Opt. Mater. Express* **1**(2), 128–137 (2011).

## 1. Introduction

Magneto-optical sensors have attracted lots of research attentions due to their many advantages including high sensitivity, high response frequency and small size as compared with their conventional competitors [1,2]. Recently, optical fiber-based magneto-optical sensors have been intensively studied by incorporating magnetic fluid [3–6], which is a novel nano-material with diverse magneto-optical effects including Faraday effect, tunable refractive index, field dependent transmission and birefringence [7,8]. By using the field dependent birefringence of magnetic fluid, an optical fiber Sagnac interferometer based magneto-optical fiber sensor has been realized [4]. By infiltrating magnetic fluid into air holes in the cladding, a short length of index-guided photonic crystal fiber was converted into photonic bandgap fiber with a tunable band gap so that magnetic field can be measured by monitoring the bandgap wavelength [3]. By surrounding a long-period fiber grating or an etched fiber Bragg grating (FBG) with magnetic fluid and measure wavelength shift of the resonance, fiber gratings have also been used for magnetic field measurement and tunable filters [5,6,9,10]. A two tilted fiber Bragg gratings (TFBGs) based ring resonance cavity structure surrounded by magnetic fluid has also been reported for magnetic field measurement, but the resonance structure based on ghost mode adds to the difficulty of fabrication and cost [11].

In this work, a magnetic field sensor based on a TFBG incorporating with magnetic fluid is proposed and experimentally demonstrated. It is well known that TFBGs belong to the short period fiber grating family but possess the sensing property of long period gratings. By tilting the grating planes related to the perpendicular of the fiber axis, they cannot only couple the light from forward propagating core mode to backward propagating core mode as normal FBGs do, but also couple the forward propagating core mode to backward propagating cladding modes [12]. This makes them more advantageous than normal FBGs in sensing applications as the exited cladding mode resonances in TFBGs are sensitive to surrounding refractive index and fiber bending [12–20]. Here we surround a TFBG with magnetic fluid whose complex refractive index is tunable with external magnetic field. By detecting variations of extinction ratio of the TFBG's cladding mode resonance and wavelength shift of the optical spectrum, simultaneous measurement of magnetic field strength and temperature is achieved.

## 2. Sensor fabrication and principle

In the experiment, the TFBG was manufactured by using phase mask method in a hydrogen-loaded Germanium-doped single-mode fiber with a frequency-doubled Argon laser emitting at 244 nm. The period of phase mask is 1080 nm. The achieved TFBG is 20-mm long with an internal tilt angle of 2 degree. A transmission spectrum can be seen in Fig. 1. The magnetic

fluid used in this experiment, EMG605 (from Ferrotec), is a water-based ferrofluid fabricated by using the chemical coprecipitation technique. It is a black-brown translucent liquid with real part in complex refractive index of around 1.41. The nominal diameter of the nanoparticles,  $\text{Fe}_3\text{O}_4$ , is 10 nm. The volume concentration is 3.9%. The magnetic susceptibility and saturation magnetization are 2.96 Gauss and 220 Gauss, respectively.

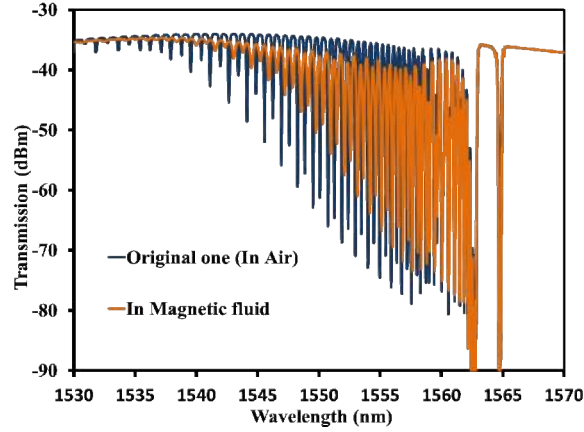


Fig. 1. Transmission spectra of the TFBG before and after magnetic fluid surrounding.

As analyzed in [12], wavelengths of the TFBG's Bragg reflection,  $\lambda_B$ , and the  $i$ th cladding mode resonance,  $\lambda_{c,i}$ , are determined by the phase matching conditions and can be expressed as

$$\lambda_B = 2n_{\text{eff},co} \Lambda / \cos \theta, \quad (1)$$

$$\lambda_{c,i} = (n_{\text{eff},co} + n_{\text{eff},cl,i}) \Lambda / \cos \theta, \quad (2)$$

where  $\theta$  is tilt angle of the grating planes related to the perpendicular of the fiber axis,  $n_{\text{eff},co}$  and  $n_{\text{eff},cl,i}$  are effective refractive index of the core mode and the  $i$ th cladding mode, respectively.  $\Lambda$  corresponds to the nominal grating period and can be described as  $\Lambda = \Lambda_g \cos \theta$ , where  $\Lambda_g$  denotes the grating period along the axis of the fiber.

When the TFBG is surrounded by magnetic fluid and external magnetic field with variable strength is applied, the effective refractive indices of cladding modes would depend on the magnetic field-induced surrounding refractive index change. The  $\text{Fe}_3\text{O}_4$  nanoparticles around the TFBG form a kind of granular metal film. Since the refractive index of metals is complex, an additional effect comes into play as the effective index of the cladding modes also becomes complex, i.e. the cladding modes become lossy [21]. The perturbation in the imaginary part of cladding modes' complex effective refractive indices will lead to the attenuation in the guiding properties of the cladding modes and reduction in amplitude of cladding mode resonances as a result [21,22]. Meanwhile, the real part of magnetic fluid's complex refractive index increases with the external magnetic field strength and the cladding mode resonances will become attenuated and gradually disappear as the modes become lossy (they are no longer totally internally reflected by the cladding boundary as its evanescent field penetrates more and more into the magnetic fluid). As a result, extinction ratio of the cladding mode resonances will decrease as the magnetic field strength increases.

The detailed complex refractive index variation mechanism of magnetic fluid under applied magnetic field can be analyzed as follows. When an external magnetic field is applied, the structural pattern state of magnetic fluid is changed from random homogenous to field dependent structural pattern. The nanoparticles in magnetic fluid agglomerate and further form chains and magnetic columns along the direction of magnetic field. Consequently, the complex dielectric constant of the magnetic fluid and hence the complex

refractive index of the magnetic fluid, especially the imaginary part, is changed [8,23]. And further research indicates that the relationship between real part in complex refractive index of magnetic fluid and external magnetic field strength follows Langevin function [24].

While environmental temperature changes, resonant wavelengths of Bragg mode and cladding modes will change due to thermal expansion and thermo-optic effects of the optical fiber. Wavelength changes of Bragg mode and the  $i$ th cladding mode can be given respectively by

$$\Delta\lambda_B = 2 \left( \frac{n_{eff,co}}{\cos\theta} \frac{d\Lambda}{dT} + \frac{\Lambda}{\cos\theta} \frac{dn_{eff,co}}{dT} \right) \Delta T, \quad (3)$$

$$\Delta\lambda_{c,i} = \left( \frac{(n_{eff,co} + n_{eff,cl,i})}{\cos\theta} \frac{d\Lambda}{dT} + \frac{\Lambda}{\cos\theta} \frac{d(n_{eff,co} + n_{eff,cl,i})}{dT} \right) \Delta T, \quad (4)$$

where  $\Delta T$  denotes the change of temperature. From these wavelength changes, temperature can be monitored simultaneously.

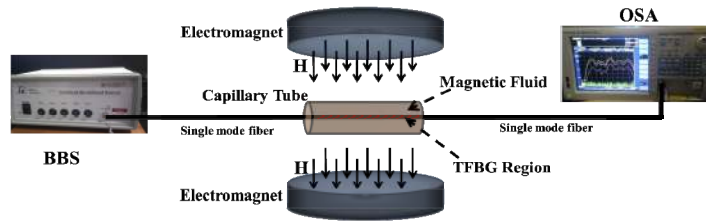


Fig. 2. Experimental setup for magnetic field measurement.

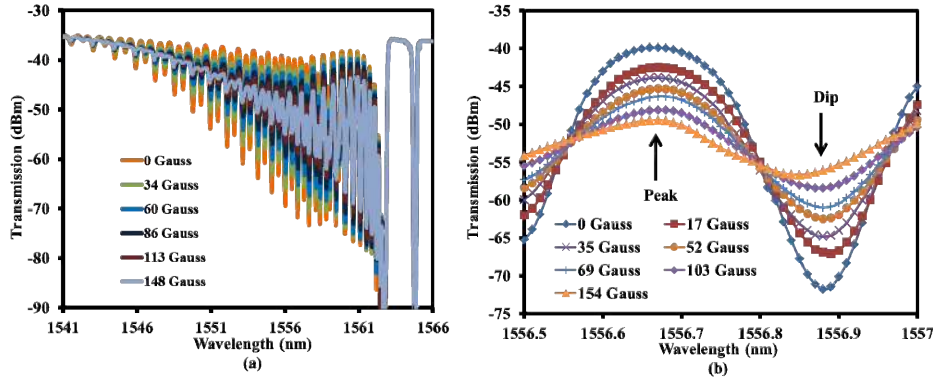


Fig. 3. (a) Transmission spectra of the TFBR under various magnetic field strengths; (b) Evolution of the selected cladding mode resonance with magnetic field.

### 3. Experimental results and discussions

Figure 2 illustrates the experimental setup for magnetic field measurement with the proposed fiber grating sensor. The TFBR was placed in a magnetic fluid-filled capillary tube with inner diameter of  $\sim 500$   $\mu\text{m}$ . A variable magnetic field was generated by an electromagnet (EM4-HVA, LakeShore) and calibrated by a gaussmeter (Model 425, LakeShore). The magnet has two poles of 10 cm diameter, and the air gap between the two poles was fixed at 15 cm in the experiment. The fiber sensor was placed in the centre of the uniform field zone and the transverse Hall probe of the gaussmeter was fixed near the sensor head. The magnetic field was applied perpendicularly to the fiber axis. Light from a broadband light source (BBS) was

launched into the sensor from the lead-in single mode fiber. Transmission spectrum of the TFBG was monitored synchronously by using an optical spectrum analyzer (OSA, AQ6370).

After surrounded by the magnetic fluid, intensity of the TFBG's cladding mode resonances, as also shown in Fig. 1, is decreased significantly as compared with that of the original one. The change in TFBG transmission spectrum is similar with that when the TFBG is deposited by metal nanoparticles reported in [22] and [25], further demonstrating that the amplitude and wavelength change of the cladding modes are caused by the complex refractive index of the covered magnetic fluid. Particularly, the reduction of the top envelope transmission spectrum after magnetic fluid surrounding is resulted from the perturbation in the imaginary part of the cladding modes' complex effective refractive indices and the scattering effect caused by the evanescent field of the cladding modes propagating through the metal nanoparticles on the optical fiber surface. The imaginary part of the complex refractive index may lead to significant attenuation in amplitude of cladding mode resonance of TFBGs (a calculated attenuation up to 17 dB is reported for imaginary part of refractive index of  $\sim 2.9 \times 10^{-4}$  for a copper nanoparticle-deposited TFBG [25]).

When the strength of the applied magnetic field was increased, it can be observed that extinction ratio of the cladding mode resonances decreases gradually with the enhancement of the magnetic field strength. Figure 3(a) shows several measured transmission spectra of the TFBG under different magnetic field strength. Because the imaginary part in complex refractive index of magnetic fluid acts the key role in changing the extinction ratio of TFBG cladding mode resonances but contributes little to TFBG spectrum wavelength shift [21]. Moreover, the scattering effect, analyzed in the last part, is also a dominant factor in the spectral attenuation of the cladding modes under the applied magnetic fields. Thus, as shown in Fig. 3(a), the extinction ratio of cladding mode resonances is modulated strongly by the external magnetic field.

It is notable that the wavelengths of cladding mode resonances are nearly not changed by the external magnetic field based on the measured results. It is reasonable since the wavelength shift is already very small when the TFBG was immersed in the magnetic fluid from air (i.e. when its surrounding refractive index was changed from 1 to 1.41), even for the highest order cladding mode, as shown in Fig. 1. So the real part of the complex refractive index of the magnetic fluid, which is changed little by the external magnetic field, has nearly no effect on cladding mode resonances wavelength-shift in the transmission of the TFBG in this case, neither the magnetic field-induced birefringence in the magnetic fluid. The fixed cladding mode resonance wavelength with magnetic field is useful for temperature referencing, which is based on wavelength monitoring.

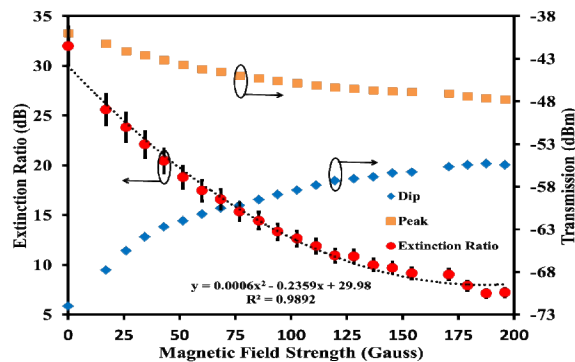


Fig. 4. Relationship between extinction ratio and magnetic field strength.

To study the relationship between extinction ratio and external magnetic field strength, we chose one of the cladding modes with resonance wavelength around 1556.8 nm to test. The zoomed transmission spectrum changes are shown in Fig. 3(b). The extinction ratio, determined as the difference between the peak power and the dip power in the transmission

spectrum, is shown in Fig. 4 as a function of magnetic field strength. The average data of extinction ratio for three measurements fit very well to quadratic function with fitting degree of 0.9892. The fitting function is  $y = 0.0006x^2 - 0.2359x + 29.98$  with  $x$  corresponding to magnetic field strength and  $y$  corresponding to extinction ratio. The variation of the results is indicated by the size of the error bars in Fig. 4 and the maximum measurement deviation (at 26 Gauss) is  $\pm 1.5$  Gauss.

For temperature measurement, we put the sensor in a thermostatic tank, changed the temperature between 20 and 60 °C with no external magnetic field applied, and recorded the wavelength shifts of the Bragg mode resonance and one of the cladding mode resonance at  $\sim 1556.8$  nm. The measurement results are shown in Fig. 5. The calculated sensitivity is 8.35 pm/°C and 8.38 pm/°C for the Bragg mode resonance and cladding mode resonance, respectively. The two values are very close and agree well to the typical temperature sensitivity of normal FBG sensors. This same sensitivity to temperature can be explained by Eqs. (3) and (4), where the difference between the wavelength shifts  $\Delta\lambda_B$  and  $\Delta\lambda_{c,i}$  is proportional to  $d(n_{eff,co} - n_{eff,cl,i})/dT$ , which is a very small factor that can be neglected. Therefore, we can measure temperature by monitoring only one of the modes. What's more, extinction ratio of the selected cladding mode resonance keeps nearly fixed when temperature changes. This means the temperature measurement will not affect the magnetic field measurement.

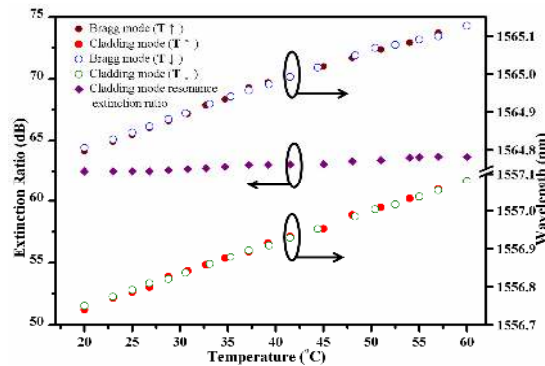


Fig. 5. Measured wavelength shifts against temperature.

#### 4. Conclusion

In summary, we have proposed a novel TFBG-based magnetic field fiber sensor by interacting magnetic fluid. Complex refractive index of magnetic fluid changes with magnetic field and thus affects guiding properties of cladding modes excited by the TFBG. By monitoring extinction ratio of TFBG's cladding mode resonance, magnetic field strength up to 196 Gauss has been successfully measured. Meanwhile, temperature measurement with sensitivity of 8.4 pm/°C has been achieved simultaneously by detecting wavelength shift of the transmission spectrum with no cross effect. The presented magneto-optical fiber sensor keeps the advantages of robustness, easy fabrication and low cost.

#### Acknowledgments

This work was supported by the National Basic Research Program of China (973 Program) under Grant No. 2010CB327804, National Natural Science Foundation of China under Grant Nos. 61007050 and 61007051, National Natural Science Foundation of Zhejiang Province, China under Grant No. Z13F050003 and Zhejiang Xinmiao Talent Project Grant No. 2012R409056.